Appendix A

Fluxgate Gradiometer

Overview

The fundamental components of a fluxgate magnetometer include the fluxgate sensor with various geometries, fluxgate electronics, and a wiring harness linking the sensor and electronics. The ensuing sections concentrate on the ring core sensor configuration due to its prevalence and efficacy (Korepanov and Marusenkov, 2012, Ripka, 1992). The ring core, a key variant of fluxgate sensors, comprises meticulously selected materials, including a permalloy ring core, sense units, and ancillary components such as circuit boards, tuning capacitors, temperature sensors, non-magnetic resistive heater tape, sensor body, and cover. Notably, the emphasis on non-magnetic materials is critical to minimizing interference with measurements. The sensitivity of the instrument relies on the unique properties of the ring core's permalloy material, characterized by high magnetic permeability and easily magnetized (Miles et al., 2019). These distinctive characteristics are the reason for the instrument's precision in measuring magnetic fields. Utilizing a solenoid created by wrapping the sense winding around a bobbin, a single sense unit discerns a specific axis during magnetic field measurements. Coupling two sense units enhances the instrument's capacity to measure two distinct axes, thereby expanding its analytical capabilities.

A.1 Operational Principles of Ring Core Fluxgates

Operational Mechanism

Fluxgate magnetometers are consistent of a soft magnetic material, like iron or iron-nickel alloys, drive coil and a sense coil. Compared to other magnetometers, the components of the fluxgate gradiometers are simple and cheap and yet construct a highly sensitive instrument, which explains why they are so prevalent in archaeological prospection. The soft magnetic material in the core of the fluxgate gradiometer must not hold remanent magnetization and should have high permeability and low coercivity (very eas-

ily magnetized and demagnetized) and this is why iron and iron-nickel alloys are used. Along the drive coil runs AC current, which in turn generates a variable with time magnetic field, along the length of the core metal. The generated magnetic field is larger than the magnetic field of Earth and its strength is so large that it brings the core metal into and out of saturation. When the drive coil magnetic field is not present then the core component of the fluxgate magnetometer is magnetized in the direction of the magnetic field. When the drive coil magnetic field increases it starts to push out the magnetic flux of Earth‘s magnetic field out of the core component and brings it into saturation (Acuña, 2002). Then the magnetic field from the drive coil decreases until it goes to 0 and the core component gets magnetized by Earth‘s magnetic field again. The same cycle is repeated but this time the drive coil magnetic field is applied in the opposite direction. As a result of the variable with time drive coil magnetic field and the Earth‘s magnetic flux being pushed in and out of the core material, a variable magnetic field is created. This variable magnetic field induces an electric field and as a result and electric current runs inside the sense coil. The electric current is proportional to the strength of the magnetic field. This is based on Maxwell-Faraday‘s law of induction:

$$\oint \mathbf{E} \cdot d\mathbf{l} = -\frac{d\Phi_B}{dt} \tag{A.1}$$

In this equation:

- $\oint \mathbf{E} \cdot d\mathbf{l}$ represents the line integral of the electric field ($\mathbf{E}$) around the closed loop of the sense coil. This integral effectively gives the total electromotive force (EMF) induced in the coil.
- $\frac{d\Phi_B}{dt}$ is the rate of change of the magnetic flux (Φ_B) through the area enclosed by the coil.

In practical terms, this means that the EMF induced in the sense coil is directly proportional to the rate of change of the magnetic flux through the coil. By measuring this EMF, the characteristics of the changing magnetic field can be deduced, which is the fundamental operating principle of the fluxgate magnetometer.

The drive winding that‘s going around the ring core is being used to drive the permalloy core material into and out of saturation. This is done by applying an alternating current. Important to note is that the permeability of the core material is going to change when it‘s saturated and when it‘s unsaturated. This change in saturation will affect the material‘s response to the background field (the magnetic field we are interested in) (Baranov et al., 2018). While the core is driven into and out of saturation that sense unit that‘s around the ring core is going to ”gate” the flux by measuring a voltage produced from the inflow and outflow of flux.

Hysteresis Loop Analysis

There are two different scenarios presented in Figure A.1 - when the permalloy material is saturated and unsaturated and each one with its corresponding hysteresis loop.

The hysteresis curves essentially show where the current is applied (Primdahl, 1979). For the case when the permalloy is out of saturation on the hysteresis loop the shaded region is where there is very little current or close to zero current applied. In this out of saturation case the permeability of the permalloy material is high and therefore the sense winding is able to detect the background field, because there is room within the material for detection.

Now we move to the saturated scenario. If we look at the hysteresis curve we are near that positive current or the negative current, but essentially we have driven that permalloy material to saturation, which means it‘s permeability is low and it cannot measure a background field. The material is essentially full when it‘s saturated so it‘s pushing out that background field, in which case it‘s visible in the figure that the background magnetic field is not being sensed by that sense coil. And as the material goes into and out of saturation by alternating the current the background field (if one is present) is going in and out of the ring core. This changing magnetic field will drive the voltage that the sense unit will be able to measure.

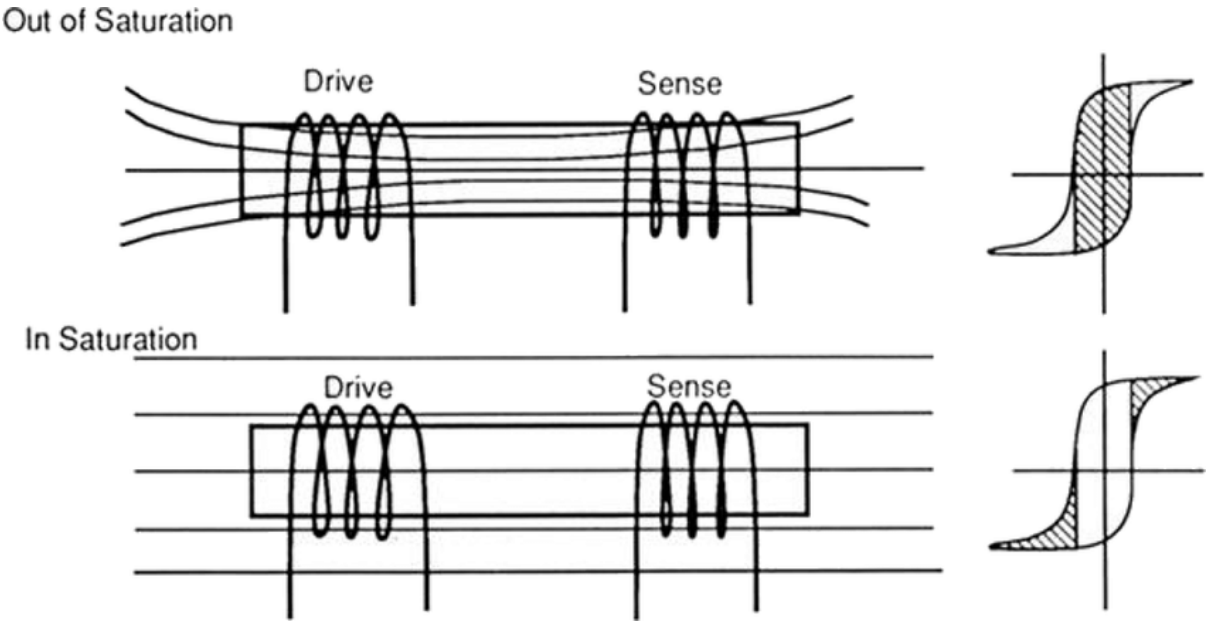

Figure A.1: Two different scenarios - when applied magnetic field causes the permalloy material to go in and out of saturation and the hysteresis loop for each case (Lenz and Edelstein, 2006).

Induction in the Sense Unit

The core component of a fluxgate magnetometer is driven in and out of magnetic saturation by an alternating current (AC). When the core is in magnetic saturation, its ability to carry additional magnetic flux is minimal. When an external magnetic field is present, it adds or subtracts to the magnetic field produced by the AC in the core. This external field causes the core to reach saturation more quickly or slowly in each cycle, depending on the direction of the external field relative to the field of the AC. According to Faraday's Law, a changing magnetic field induces an electromotive force (EMF) in a nearby conductor. In a fluxgate magnetometer the sense coils are wound around the core. As the core enters in and out of saturation, the magnetic field through the sense

coils changes rapidly(TUMANSKI, 2013). The changing magnetic field through the coils induces a voltage in them by electromagnetic induction (as per Faraday's Law). This induced voltage changes in a way that is asymmetric within each cycle of the AC, due to the influence of the external magnetic field. Meaning, that because of the influence of the external magnetic field, the induced voltage in the coils no longer remains symmetric within each cycle. Instead, the pattern of the voltage changes in an asymmetric manner. For instance, if the external magnetic field makes the core reach saturation quicker in one half of the AC cycle than the other, the induced voltage will peak earlier in that half of the cycle, leading to an asymmetrical voltage waveform. The strength and direction of the external magnetic field is determined through the voltage produced inside the sense coils.

A.2 Geometry of Fluxgate Magnetometers

Evolution of Geometry

The geometry of the fluxgate core and its drive winding matters. In the simple case that was discussed previously was essentially looked at a single solenoid (Figure A.2). Now taking it a step further in talking about the geometry a square bobbin can be introduced (Can and Topal, 2015). In this square bobbin a split in the drive winding is created. The wire that goes around the square bobbin is a single drive winding. In this case it is oriented in a way that when the current is applied in either direction the magnetic fields generated will be antiparallel to each other (Figure A.3).

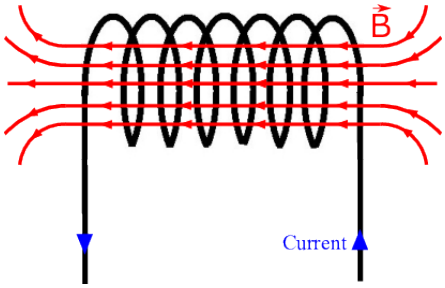

Figure A.2: Single solenoid through which when a current is applied a magnetic field is generated based on the right-hand rule (https://cds.cern.ch/record/2791844/plots).

Multiaxis Measurement

The Figure A.4 is displaying the waveforms for a single solenoid, a split drive winding without an external field and a split drive winding with an external field. The drive waveforms for the two halves are equal in amplitude but opposite in sign and when there is no external field they will cancel out. What that means is that the sense winding is not going to be sensitive to the magnetic field generated by the alternating current because the two halves of the drive winding will be generating fields which cancel each other out. This allows the sensor, if it's in the presence of a background field, to measure it and in this case the drive waveform will be shifted in the direction of that background field. The wave form is shifted in the direction and the values of the background field.

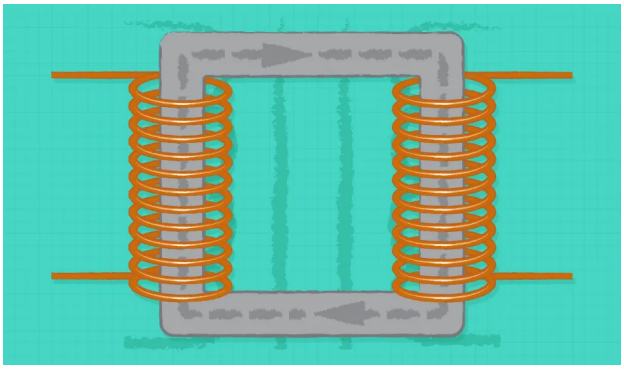

Figure A.3: Square bobbin with a split in the drive winding. It is oriented so when the current is applied in either direction it generates a magnetic fields that are antiparallel to each other (https://www.cui.com/blog/isolated-vs-non-isolated-power-converters).

Beyond Square Configurations

This goes to show that we can utilize a different geometry in the core of the fluxgate in order to measure the background field of interest (Djamal et al., 2011). And if we want to take it one step further and instead of splitting the drive winding just on two sides of the square, let's split the drive winding on all four sides of a square bobbin. Having gotten to this point one can imagine how the next step would be to create simply the geometry of a ring core with infinitely many sides which oppose each other - ring-core bobbin with windings helically wrapped around it.

Multiaxis Measurement with Redundancy

This geometry of the drive coil (Primary coil) allows the sense coil (Secondary coil) to detect a background field, however only the component of a background field which is in direction perpendicular to the direction of the windings of the sense coil (Figure A.5). Including two ring core sense unit combinations (each measuring in two perpendicular to each other directions i.e. x-y and y-z) on a fluxgate allows for measurement in three axes with one being redundant. In this case x, y and z directions will be measured, however y-direction is measured twice and that is why it is called redundant. This configuration of two sense units allows to create a fluxgate magnetometer which measures in 3D.

A.3 Fluxgate Gradiometer

The fluxgate gradiometers are sensitive with respect to direction, which means that they do not measure the absolute value of the magnetic field, but each sensor measures just one of its components. The fluxgate gradiometer is a combination of two fluxgate magnetometers, each of which measures the value of the magnetic field along of the the axes (in this case z-axis), aligned along the same axis and separated at a certain distance. Most importantly that distance does not change, because we are interested not only in the measurements from the two magnetometers, but rather the differential measurement

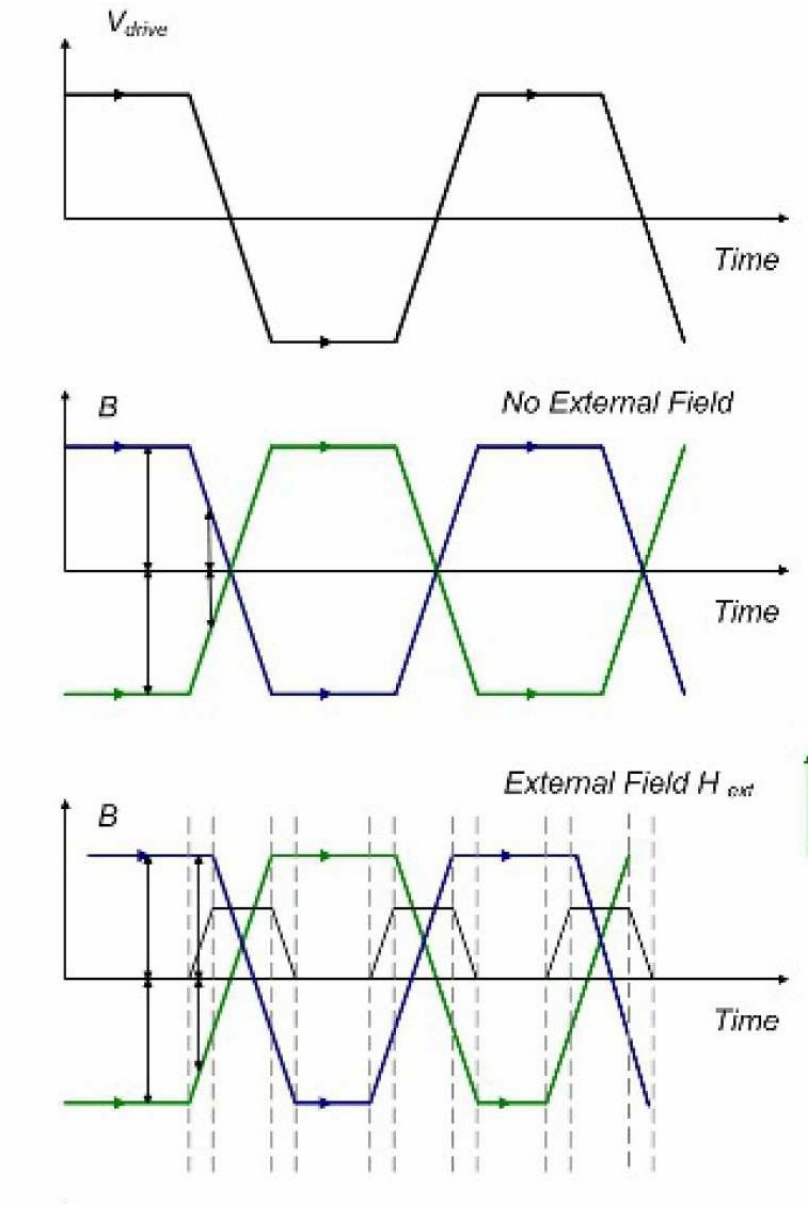

Figure A.4: The input waveforms, which bring the permalloy material into saturation. The top graph displays the waveform for a single rod. The second one - for two opposing rods, where the saturating magnetic fields are equal but with opposite directions (without an external magnetic field to measure) and cancel each other out. The third graph shows the two saturating magnetic fields as well as the external field H_{ext} (https://www.imperial.ac.uk/space-and-atmospheric-physics/research/areas/space-magnetometer-laboratory/space-instrumentation-research/magnetometers/fluxgate-magnetometers/how-a-fluxgate-works/).

mid way along the axis (Figure A.6). This type of measurement gives the gradient of the magnetic field (therefore a gradiometer), rather than an absolute measurement, like a traditional fluxgate magnetometer.

A magnetometer that measures the absolute value of the magnetic field along a certain axis and records a signal, which is a composite of Earth‘s magnetic field and every other source in the vicinity of the magnetometer. The gradiometer however measures the

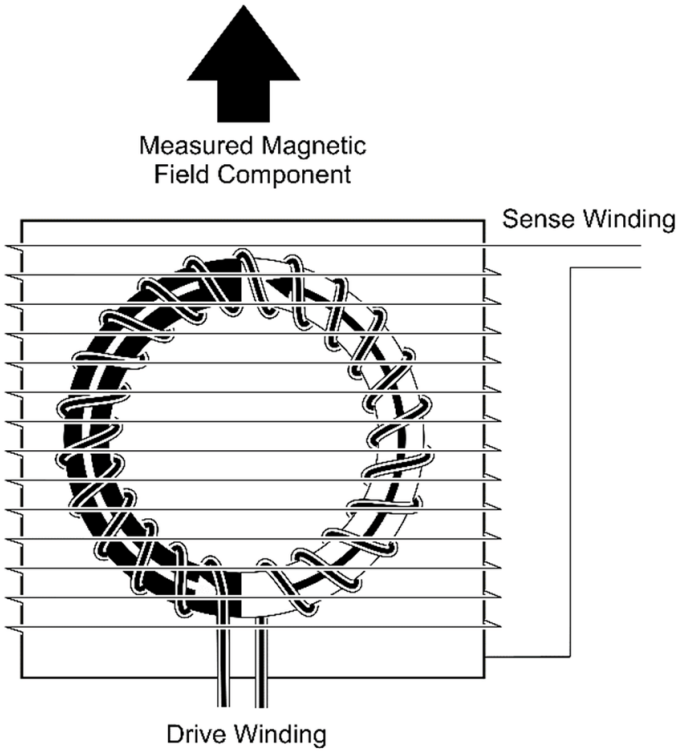

Figure A.5: Schematic of a fluxgate magnetometer.The ring core is on the inside, surrounded by the sense windings. This fluxgate magnetometer detects magnetic fields in a direction perpendicular to the direction of the windings (Miles et al., 2017).

difference in the magnetic field between its two sensors. By taking the difference in measurements, the instrument is able to determine the gradient of the magnetic field along the axis between the sensors. The magnetic field gradient is calculated by subtracting the magnetic field measured by one sensor from the magnetic field measured by the other sensor, and then dividing by the distance between the sensors. This gives the gradient in units of magnetic field change per unit distance [nT/m]. Because the gradiometer makes differential measurements therefore it is more sensitive to local magnetic sources and less so to the wide variations of Earth‘s magnetic field (Bichurin et al., 2021). This makes them particularly useful for archaeological applications where small, local anomalies are of interest. In archaeology a fluxgate gradiometer can detect the presence of pits, ditches, walls and other archaeological features based on the strength of their magnetic field with respect to the local magnetic field. These signals are too subtle to be detected by a standard magnetometer but can be picked up as a gradient by a gradiometer.

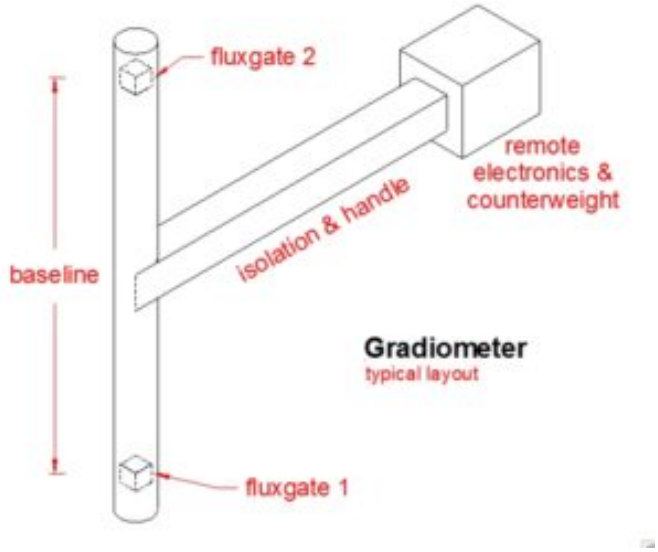

Figure A.6: Schematic of a fluxgate gradiometer. The two fluxgate sensors are aligned along an axis and separated at a certain baseline distance. They are fix with a tube from a non-magnetic material. The electronics and counter weight must also be separated with a non-magnetic material, so as not to disturb the measurements (https://popularelectronics.technicacuriosa.com/2017/03/16/inside-the-fluxgate-gradiometer/).

Appendix B

Cesium Vapor Magnetometer

Scalar magnetometers are instruments, which measure the total strength of the magnetic field, unlike vector magnetometers, which provide information on the field's direction. The optically pumped alkali metal vapor magnetometers are a type of scalar magnetometers. This type uses the properties of alkali metals like cesium, potassium, and rubidium for the detection of the magnetic field's strength. These metals, all situated in the first column of the periodic table, have only one electron in their outermost shell, which makes them sensitive for the detection of magnetic fields (Figure B.1).

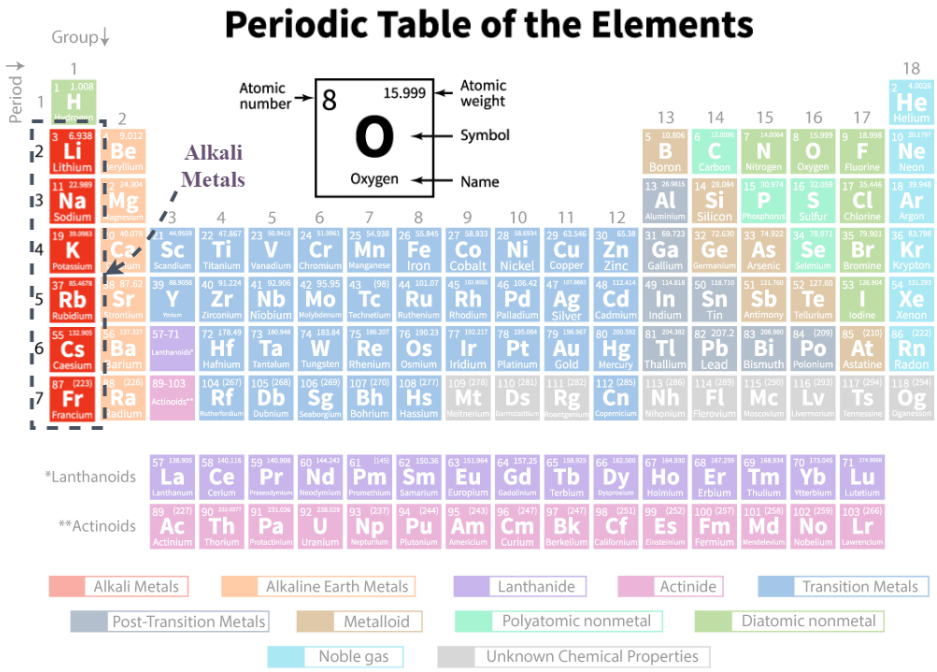

Figure B.1: The Alkali metals are indicated. Being in the first column means they have a single electron in their outermost shell and that is why they are used in the manufacturing of optically pumped magnetometers (https://www.geeksforgeeks.org/alkali-metals/).

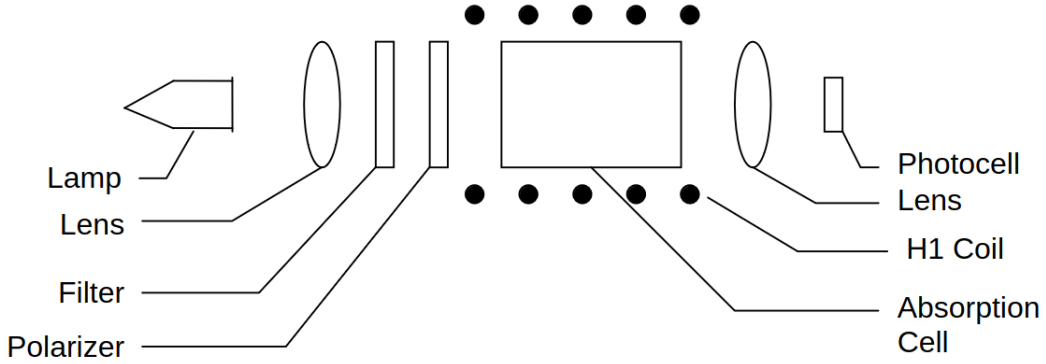

Figure B.2: The Alkali metals are indicated. Being in the first column means they have a single electron in their outermost shell and that is why they are used in the manufacturing of optically pumped magnetometers (*G-822A and G-823A & B Cesium Magnetometer Operation Manual*, 2004).

B.1 Cesium Vapor Magnetometer Design

The cesium magnetometer is an instrument that measures the absolute value of the magnetic field. It‘s design is based on the principles of optical pumping and magnetic resonance. It takes advantage of the cesium atom‘s atomic structure, which has a single electron in its outermost shell. It‘s response to light and magnetic fields allows it to accurately detect and measure the strength of the magnetic fields. The instrument itself consists of a cesium spectral lamp, absorption cell containing cesium vapor, circular polarizer, photodetector and magnetic field coils (Figure B.2).

The cesium spectral lamp emits many spectral lines, but only one in the infrared spectrum is utilized for the magnetometer. There are two lenses which are situated on opposite sides of the absorption cell. One of the lenses is placed after the lamp and the other one is placed before the photodetector. The one after the lamp bends the light to parallel rays and the one before the photodetector focuses the light rays on it. The filter has the function to pass light with only specific wavelength 894.1 nm. The purpose of that light will be to excite the electrons of the cesium atoms inside the absorption cell to higher energy states. After passing through the polarizer the light becomes circularly polarized, either right-hand or left-hand. The direction of polarization will control the orientation of the electrons spins in the cesium atoms, which are aimed to be aligned during the optical pumping. The core of the magnetometer is the absorption cell, which contains the cesium vapor, as well as a buffer gas - either helium or nitrogen. The purpose of the buffer gas is to stabilize the cesium vapor and reduce collisional broadening of the atomic spectral lines. Another element of the magnetometer is the H1 coil. It‘s purpose is to introduce an oscillating magnetic field H1 at and around the Larmor frequency for the field that is being measured. The last component is the photocell (photodetector), which receives the light passed through the absorption cell. The intensity of the light being emitted from the lamp is known, therefore by detecting the intensity of the light which falls on it, the photocell can determine the transparency of the gas in absorption cell, or rather how the transparency changes. This transparency is important, because it relates

to the Larmor frequency of the ambient magnetic field, and from there the strength of the magnetic field itself.

In principle, the light being shone on the cesium gas, has a specific wavelength, therefore a specific energy and is right-hand circularly polarized, in order to create a population imbalance in the different energy sublevels. This process leads to the increase of the transparency of the cesium vapor. After that an oscillating field (H1), which frequency increase with time, is applied to the gas. This field has the effect of scrambling the the electrons between the different energy sublevels, which leads to a decrease of the gas transparency. The frequency of the field which accomplishes this is called the Larmor frequency. The Larmor frequency is proportional to the ambient field. And that is how Earth's magnetic field is determined.

B.2 Principles of Optical Pumping

For the purposes of this magnetometer ^{133}Cs is used. As mentioned previously, the alkali metals, such as Cs, have a single electron in their outermost shell and that makes them perfect candidates. The ground state of the electron in the outermost shell is $6S_{1/2}$ and the excited state is $6P_{1/2}$ (Figure B.3). The difference in energy between those two levels is the energy carried by the filtered, right-hand polarized light from the cesium lamp (D1 = 894.1nm). There is another excited state of the for the electron - $6P_{3/2}$ and it is achieved by shining a light with a different wavelength (D2 = 852nm). However for this magnetometer, a D1 spectral line light is used.

The ground state ($6S_{1/2}$) and the excited state ($6P_{1/2}$) of the electron are each split into two levels. This splitting occurs as a result of the interaction between the nuclear spin (I) and the spin of the electron (S). The value of total angular momentum is the vector sum of the angular momenta of the nucleus and the electron. The nuclear spin quantum number (I) is 7/2 and it is the same for all cesium atoms. While the electron spin can take one of two values, either +1/2 (spin up) or -1/2 (spin down).

$$F = |I + S| = |7/2 + 1/2| = 4 \tag{B.1}$$

$$F = |I - S| = |7/2 - 1/2| = 3 \tag{B.2}$$

The different values of the total angular momentum are called hyperfine energy levels - F=3 and F=4 (Figure B.3). And to be more exact, the ground state of the electrons in the outer shell is $|6S_{1/2}, F = 4\rangle$. When it absorbs energy from incoming photons and gets excited, it goes up to a state $|6P_{1/2}, F = 3\rangle$ (SamerIAfach, 2014). In reality, the transition occurs between the different hyperfine structures of the ground state and the excited state. However for the purpose of this magnetometer a transition will be considered only between the different levels of the fine structure, because the energy from the light is 6 orders of magnitude greater than the energy between the hyperfine levels of the $6S_{1/2}$ and $6P_{1/2}$ states.

In the absence of an external magnetic field the atoms of the cesium atom would have degenerate hyperfine energy levels, which means they all have the same energy. However when an external magnetic field is introduced, like Earth's magnetic field in this case, a fenomenon called Zeeman splitting occurs and the hyperfine energy levels get divided into even smaller sublevels. The number of sublevels in each hyperfine level is determined by the value of the total angular momentum F and is equal to 2F+1. Each sublevel is indicated by a quantum number m_F, which ranges from -F to +F. Therefore the sublevels within F=3 range from [-3, 3] and within F=4 they range from [-4, 4] (SamerIAfach, 2014), as is shown in Figure B.3. The particular quantum number m_F of sublevel shows the relative orientation of the angular momentum vector of an electron in that sublevel with respect to the external magnetic field (the one that caused the Zeeman splitting). Figure B.5 shows how when Zeeman splitting has occurs in a hyperfine level F=3, electrons in situated in the different sublevels will be oriented with repsect to the external magnetic field. In the figure the direction of the magnetic field will be along the z-axis (Bai et al., 2023). The sublevel with the highest positive quantum number (m_F=3) is orietnted the closest to the magnetic field. The one with m_F=-3 is 180 degrees on the opposite side and the m_F=0 sublevel is 90 degrees away from the axis of the magnetic field. The more the magnetic field increases the closer sublevels with quantum numbers 3 and -3 will move towards the magnetic field axis, but for small fields as the one we are measuring they will never align with the axis.

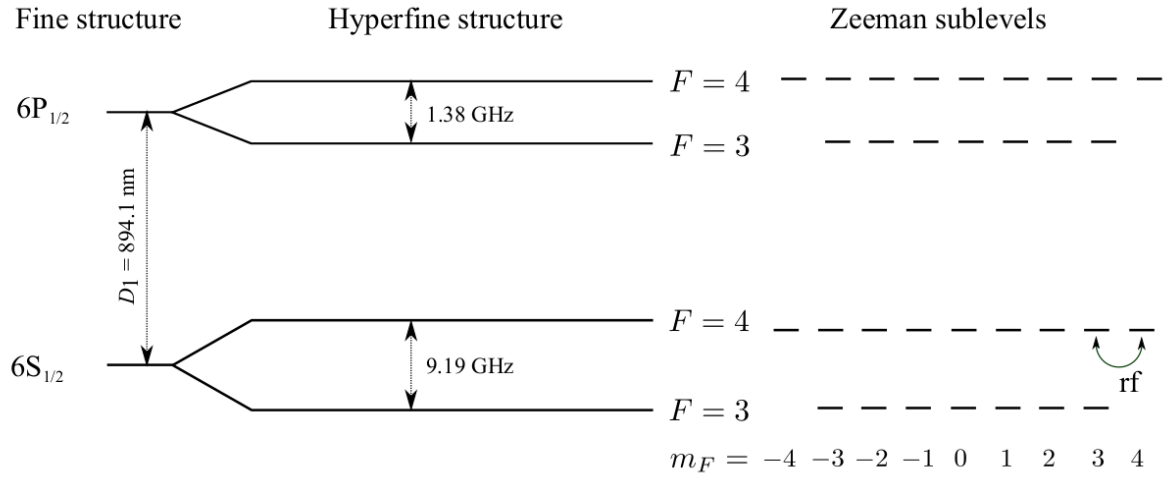

Figure B.3: Diagram of the fine and hyperfine structure of the two outer shells of cesium, as well as the sublevels created through the process of Zeeman splitting (SamerIAfach, 2014).

Each sublevel within the hyperfine level has an energy (E_{Zeeman}) determined by the quantum number of the sublevel (m_F) as well as the strength of the magnetic field, which was the cause of the Zeeman splitting (Lu et al., 2023b).

$$E_{Zeeman} = g_F \mu_B m_F B \tag{B.3}$$

g_F is the Landé g-factor for the hyperfine level, μ_B is the Bohr magneton, m_F is the magnetic quantum number, and B is the external magnetic field strength. It is important to note that the energy difference between each two adjacent sublevels of a hyperfine level is always the same, at least always for cases like this one, when the Zeeman splitting is

caused by the Earth's magnetic field, which can be considered to have relatively small strength. The energy difference between the adjacent sublevels is proportional to Earth's magnetic field and both of them are proportional to a variable called Larmor frequency (f_L). This is the frequency with which an electron situated in any one the energy sublevels precesses around the magnetic field (Figure B.4), which has cased the Zeeman splitting. The Lamrmor frequency and it's relation to the external magnetic field (B) and the energy difference between the adjacent sublevels (ΔE) is an important concept for understanding the working principle of the cesium vapor magnetometer.

The Larmor frequency (f_L) and its relation to the magnetic field (B) is given by:

$$f_L = \frac{\gamma}{2\pi} B \tag{B.4}$$

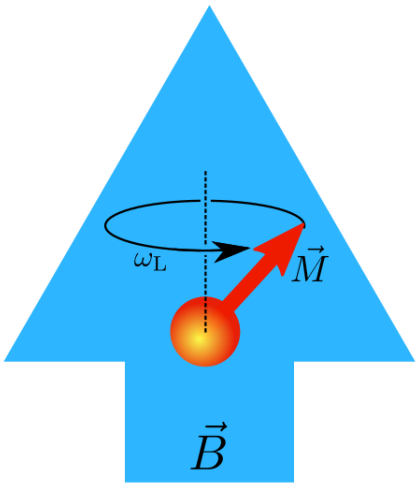

Figure B.4: Diagram that shows the Larmor frequency that occurs when an external field is present (SamerIAfach, 2014).

where γ is the gyromagnetic ratio, relating the magnetic moment (μ) to the angular momentum (L). The Larmor frequency is connected to the energy difference (ΔE) between two adjacent magnetic sublevels within a hyperfine level:

$$\Delta E = h f_L \tag{B.5}$$

where h is Planck's constant. Combining the two equations, we obtain:

$$\Delta E = h \left(\frac{\gamma}{2\pi} B \right) \tag{B.6}$$

B.2.1 Process of Spin Alignment and Population Imbalance

The ultimate goal is to determine the Larmor frequency of the electrons and from there find the value of Earth's magnetic field which caused it. The next step would be to create a population imbalance and align the spins, all in one step. This will be accomplished with

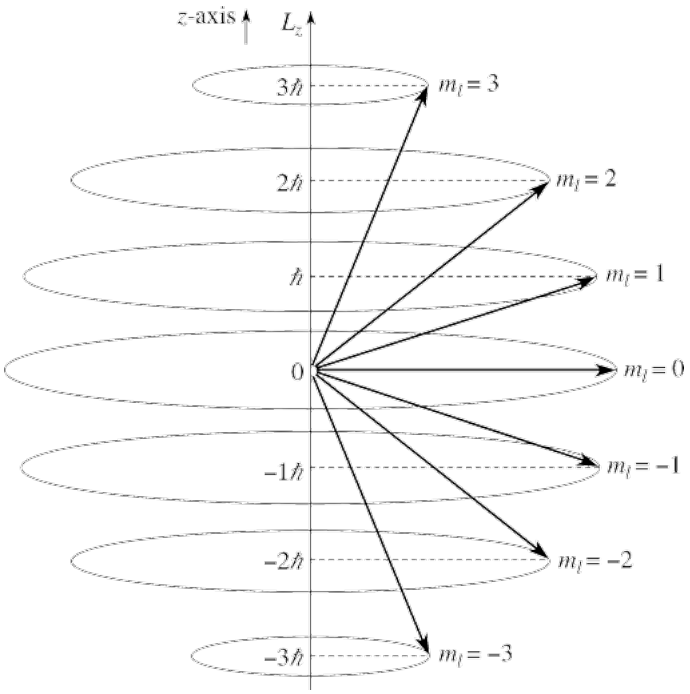

Figure B.5: Diagram of the Zeeman splitting of the hyperfine level into sublevels, due to the presence of an external field (www.met.reading.ac.uk/pplato2/h-flap/phys11_3.html).

the right-hand polarized infrared light. Before the application of the light, the cesium valance electrons are distributed randomly between the different sublevels. If there is no outside energy being introduced into the system, then the probability of an electron being in any one of the sublevels is the same. Since the sublevels throughout all the atoms are evenly occupied by electrons, this means that the transparency of the vapor is as low as it can be (the light from the lamp is absorbed by the vapor). As previously mentioned the ground state of the electrons in all the atoms is $|6S_{1/2}, F = 4\rangle$. When the circularly right-hand polarized light is applied to the vapor, the atoms absorb the energy from the photon, move to an excited state $6P_{1/2}$ and increase their quantum number m_F by one to conserve angular momentum. This excited state is not energetically stable and the electron releases energy in the form of a photon, after which it returns to its ground state, where its quantum number m_F can stay the same or change by ± 1 (Figure B.6) (Fabricant et al., 2023).

This cycle is repeated many times - the electron absorbs a photon, it gets excited and increases its quantum number by one and when it returns to the ground state, there is a probability to increase its quantum number again. Over time a population bias starts to form and the sublevels with higher quantum numbers get preferentially populated with respect to the other sublevels. Figure B.7 perfectly illustrates the effect of the applied light. Before the light is applied, the electron of each atom has an equal probability of being in any of the sublevels of the ground state. Each sublevel is more or less equally occupied. In this instance the cesium vapor is not very transparent, because there are a lot of atoms who can absorb energy and the intensity of the light from the lamp is attenuated by the cesium vapor. Over time however, through many cycles excitation and spontaneous decay of the electrons, they occupy preferentially the sublevels with higher quantum numbers. These cycles continue until no more energy can be absorbed by the electrons, because they are in the highest energy state (dark state). When this happens,

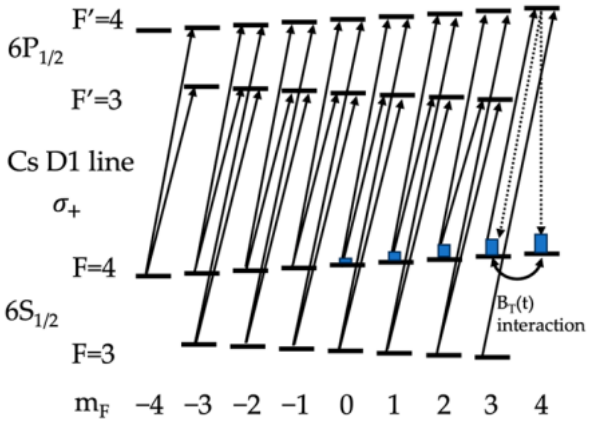

Figure B.6: Excitation of electrons with a right-hand circularly polarized infrared light. Population imbalance is created (Lu et al., 2023a).

the light from the lamp no longer can be absorbed and passes through the vapor. This is the point when the vapor‘s transparency is at its highest (Figure B.8).

The light is the most crucial component in this step. It serves a double function. It excites the electrons to a higher energy state though the energy it carries, based on its particular wavelength (894.1nm). The second function is to create a population imbalance and redistribute the electrons from the lower energy sublevels to the higher ones. This is accomplished through its polarization. It is circularly right-hand polarized, because of which, each excitation of the electron leads also to an increase of its quantum number, which occurs because of the conservation of momentum law. The light could be right-hand circularly polarized, or left-hand. The two types will redistribute the electrons in different sublevels. The right-hand polarized light will distribute them in the sublevels with higher quantum numbers (m_F=2, 3, 4), while the left-hand polarized light will accomplish the opposite (m_F=-2, -3, -4) (SamerIAfach, 2014).

B.3 Resonance Detection

The final step would be to undo the effect of the light pumping and redistribute the electrons through the sublevels randomly. The purpose of creating a population imbalance among the sublevels and then undoing it is to determine what kind of energy is needed to be introduced to the electrons in order for them to overcome the energy barrier and leave the sublevels they are currently occupying. For the purpose, the last component of the magnetometer will be utilized - the H1 magnetic field coils. They generate a transverse oscillating magnetic field which oscillates in resonance with the magnetization precession of the polarized cesium atoms. This occurs when the frequency of the oscillating magnetic field and the Larmor frequency are the equal.

The problem is that the actual Larmor frequency at any point of measurement is unknown, because it depends on the magnetic field at that point and it is also unknown. In order to determine the Larmor frequency, the oscillating magnetic field is tuned to

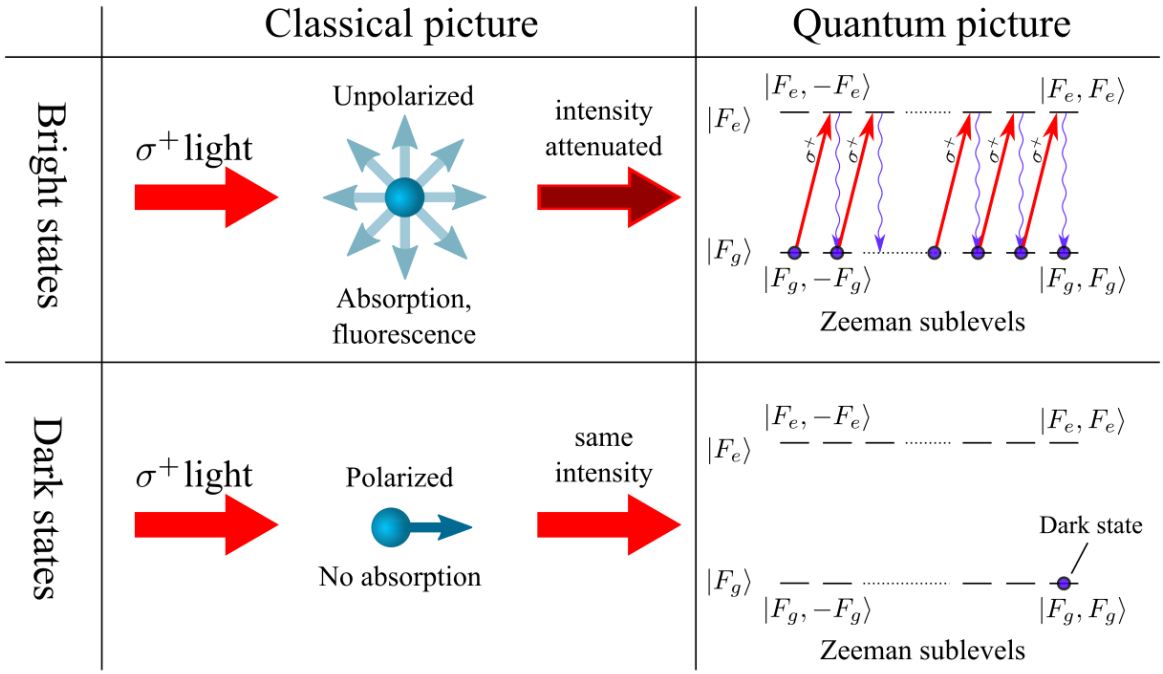

Figure B.7: The diagram shows the before and after picture of the whole system. Before the light is applied, all the electrons are randomly oriented (unpolarized) and because there are so many of them to absorb the energy from the photons, that leads to the light being attenuated from the vapor and the photodetector registers low intensity of the light. After the light has been applied, most if not all of the electrons are aligned. They are in their highest energy states and cannot absorb more energy, which leads to the photons passing through the vapor. In that case the intensity if the light is the same as it was when it was emitted (SamerIAfach, 2014).

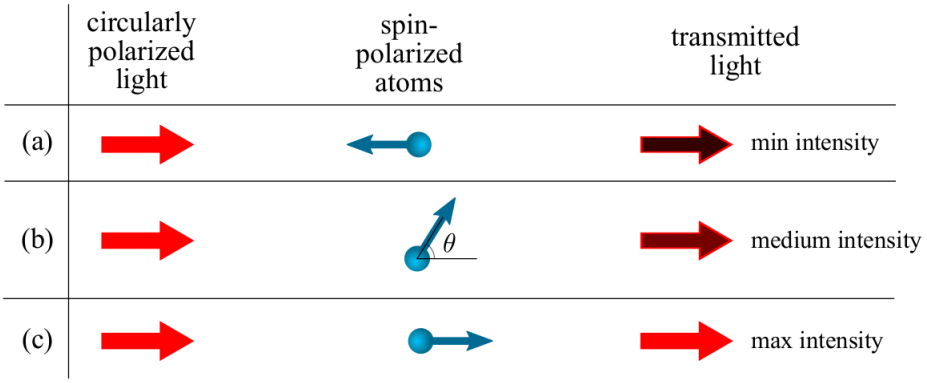

Figure B.8: Change of the intensity of the light passed through the vapor based on the polarization of the atoms. **(a)** When they are polarized in a direction opposite to the direction of the light polarization, then the transparency of the vapor is the least and the transmitted through the vapor light has a minimum intensity. **(b, c)** The more the direction polarization of the atoms matches the direction of polarization of the light the more light will be transmitted through the vapor and its transparency will increase (SamerIAfach, 2014).

a certain low frequency and over time it is slowly increased until the frequency of the oscillating magnetic field and the Larmor frequency start to resonate. This technique is called frequency sweeping. To ensure that the range of frequencies which are being cycled

through actually contain the Larmor frequency, the strength of the Earth‘s magnetic field is considered. The strength of Earth‘s field is in the range 25 000 - 65 000nT. If a range of frequencies is selected, to cycle through, which correspond to a field with strength in the 18 000 - 95 000nT range, then for certain the Larmor frequency will fall within this range.

Cycling through the range of frequencies of the H1 magnetic field starting from the lowest boundary, at first nothing will happen. Field with lower Larmor frequency and therefore not high enough energy cannot affect the electrons distribution. The transparency of the cesium vapor is high and light is passing almost completely through the vapor, without being attenuated. The detector registers high intensity light. When increasing the frequency of the oscillating magnetic field over time, its frequency will reach the Larmor frequency. At that point, enough energy will be introduced to the electrons and they will jump out of their current sublevels and start redistributing themselves through all sublevels with equal probability. When the lower sublevels start being occupied the polarized light from the lamp will once again start to get absorbed by the cesium atoms. This absorption will lead to a decrease in the transparency of the vapor and therefore a decrease in the intensity of the light registered by the photocell. These changes of the transparency of the gas will proceed until it returns to the initial state. The magnetometer uses these changes in absorption and transparency as feedback. The frequency of the H1 field at which maximum change in absorption and transparency occur, corresponds to the Larmor frequency. As previously mentioned in Formula B.4 there is a relation between the strength of the magnetic field of Earth and the Larmor frequency. If the Larmor frequency is known, considering that for cesium the gyromagnetic ratio is $\gamma_{Cs} = 2\pi \times 3.5$ Hz/nT (Lu et al., 2023a), the strength of Earth‘s magnetic field can be determined.

Bibliography

Acuña, M. H. (2002). Space-based magnetometers. *Review of Scientific Instruments*, *73*(11), 3717–3736. https://doi.org/10.1063/1.1510570

Bai, X., Wen, K., Peng, D., Liu, S., & Luo, L. (2023). Atomic magnetometers and their application in industry. *Frontiers in Physics*, *11*, 1212368. https://doi.org/10.3389/fphy.2023.1212368

Baranov, P. F., Baranova, V. E., & Nesterenko, T. G. (2018). Mathematical model of a fluxgate magnetometer. In V. Borikov, S. Uchaikin, P. Baranov, V. Ivanova, A. Dolgih, I. Minin, & O. Minin (Editors), *Matec web of conferences* (Page 01006, Volume 158). https://doi.org/10.1051/matecconf/201815801006

Bichurin, M., Petrov, R., Sokolov, O., Leontiev, V., Kuts, V., Kiselev, D., & Wang, Y. (2021). Magnetoelectric magnetic field sensors: A review. *Sensors*, *21*(18), 6232. https://doi.org/10.3390/s21186232

Can, H., & Topal, U. (2015). Design of ring core fluxgate magnetometer as attitude control sensor for low and high orbit satellites. *Journal of Superconductivity and Novel Magnetism*, *28*(3), 1093–1096. https://doi.org/10.1007/s10948-014-2788-5

Djamal, M., Sanjaya, E., Yulkifli, & Ramli. (2011). Development of fluxgate sensors and its applications. *2011 2nd International Conference on Instrumentation, Communications, Information Technology, and Biomedical Engineering*, 421–426. https://doi.org/10.1109/ICICI-BME.2011.6108590

Fabricant, A., Novikova, I., & Bison, G. (2023). How to build a magnetometer with thermal atomic vapor: A tutorial. *New Journal of Physics*, *25*(2), 025001. https://doi.org/10.1088/1367-2630/acb840

G-822a and g-823a & b cesium magnetometer operation manual (Rev. B) [Geometrics]. (2004). https://www.geometrics.com/wp-content/uploads/2018/10/MAN822AO_revB5.pdf

Korepanov, V., & Marusenkov, A. (2012). Flux-gate magnetometers design peculiarities. *Surveys in Geophysics*, *33*(5), 1059–1079. https://doi.org/10.1007/s10712-012-9197-8

Lenz, J., & Edelstein, S. (2006). Magnetic sensors and their applications. *IEEE Sensors Journal*, *6*(3), 631–649. https://doi.org/10.1109/JSEN.2006.874493

Lu, Y.-T., Liu, L.-S., Shi, Y.-Q., Zhao, T., Zhu, W.-H., Zhang, T.-F., Liu, W.-M., & Zhang, X.-J. (2023a). A High-Sensitivity Cesium Atomic Magnetometer Based on A Cesium Spectral Lamp. *Applied Sciences*, *13*(14), 8225. https://doi.org/10.3390/app13148225

Lu, Y., Zhao, T., Zhu, W., Liu, L., Zhuang, X., Fang, G., & Zhang, X. (2023b). Recent progress of atomic magnetometers for geomagnetic applications. *Sensors*, *23*(11), 5318. https://doi.org/10.3390/s23115318

Miles, D. M., Ciurzynski, M., Barona, D., Narod, B. B., Bennest, J. R., Kale, A., Lessard, M., Milling, D. K., Larson, J., & Mann, I. R. (2019). Low-noise permalloy ring cores for fluxgate magnetometers. *Geoscientific Instrumentation, Methods and Data Systems*, *8*(2), 227–240. https://doi.org/10.5194/gi-8-227-2019

Miles, D. M., Mann, I. R., Kale, A., Milling, D. K., Narod, B. B., Bennest, J. R., Barona, D., & Unsworth, M. J. (2017). The effect of winding and core support material on the thermal gain dependence of a fluxgate magnetometer sensor. *Geoscientific Instrumentation, Methods and Data Systems*, *6*(2), 377–396. https://doi.org/10.5194/gi-6-377-2017

Primdahl, F. (1979). The fluxgate magnetometer. *Journal of Physics E: Scientific Instruments*, *12*(4), 241–253. https://doi.org/10.1088/0022-3735/12/4/001

Ripka, P. (1992). Review of fluxgate sensors. *Sensors and Actuators A: Physical*, *33*(3), 129–141. https://doi.org/10.1016/0924-4247(92)80159-Z

SamerIAfach. (2014). *Developement of a cesium vector magnetometer for the neutron edm experiment* [Doctoral dissertation, ETH ZURICH] [Additional information, if any].

TUMANSKI, S. (2013). Modern magnetic field sensors – a review.